Characterization and Catalytic Studies on Defect Sites Formed upon the Thermal Decomposition of Sodium Ionic Clusters in NaX Zeolite

ARTICLE *in* THE JOURNAL OF PHYSICAL CHEMISTRY · MARCH 1995

Impact Factor: 2.78 · DOI: 10.1021/j100013a047

3 AUTHORS, INCLUDING:

John C Edwards
Independent Researcher
74 PUBLICATIONS **918** CITATIONS
SEE PROFILE

Steven L Suib
University of Connecticut
652 PUBLICATIONS **15,457** CITATIONS
SEE PROFILE

Characterization and Catalytic Studies on Defect Sites Formed upon the Thermal Decomposition of Sodium Ionic Clusters in NaX Zeolite

Mark W. Simon,[†] John C. Edwards,[‡] and Steven L. Suib*[,†,§]

U-60, Department of Chemistry, University of Connecticut, Storrs, Connecticut 06269-3060; Texaco, Inc., Texaco Research and Development, P.O. Box 509, Beacon, New York 12509; and Department of Chemical Engineering and Institute of Materials Science, University of Connecticut, Storrs, Connecticut 06269-3060

Received: October 20, 1994[⊗]

Sodium ionic clusters have been prepared by chemical vapor deposition of sodium metal at 225 °C and 1×10^{-4} Torr in NaX zeolites. A maximum loading of approximately 1.2 wt % sodium was vaporized onto dehydrated NaX zeolite. Ionic clusters prepared in this study have been determined to have the formula Na_6^{5+}. In this complex the sodium ions are arranged in octahedral geometries in the sodalite cages of NaX zeolite. Identification of these species was accomplished by electron paramagnetic resonance, magic angle spinning nuclear magnetic resonance. Fourier transform infrared spectroscopy, luminescence spectroscopy, and X-ray diffraction experiments. These ionic clusters have a localized electron trapped in the center of the octahedra, giving rise to a color center. Infrared analysis of pyridine adsorption onto NaX and NaX exposed to sodium vapor (Na(v)/NaX) revealed that initial Brønsted acidities of untreated NaX zeolites are low and that a complete loss of Brønsted acidity is observed upon treatment with Na vapor. The catalytic properties of materials exposed to sodium vapor have been studied in isomerization reactions. Defect sites or holes on framework oxygen sites are proposed as the source of catalytic activity at elevated temperatures (>340 °C). A catalytic mechanism for isomerization of cyclopropane to propylene over positively charged defect sites associated with Na_6^{5+} clusters in Na(v)/NaX zeolites is discussed. Activation energies, based on Arrhenius plots for first-order reactions, and rates of propylene formation are determined for cyclopropane isomerization reactions over defect sites in Na(v)/NaX catalysts. Two reaction pathways are proposed for the treatment of sodium vapor on these materials. The dominating reaction produces Na_6^{5+} clusters in the sodalite cages of NaX zeolites. In a second reaction, Na vapor reduces Brønsted acid sites on terminal hydroxyl groups. The latter reaction leads to the formation of hydridic species on framework silicon atoms at high temperatures and the generation of electron holes on framework oxygen. Activation of defect sites has been observed only at high temperatures. Electron paramagnetic resonance studies show that naphthalene, sublimed on defect sites, results in the formation of naphthalene radicals.

I. Introduction

The use of sodium vapor to generate catalytically active species in zeolites is highly unusual. Sodium and other metals like vanadium, copper, and nickel, which are found in heavy hydrocarbon feed stocks, usually act as poisons in fluid cracking catalysts.[1] Several studies have shown that increased concentrations of sodium in zeolites are directly related to a decrease in the catalytic activity of these materials.[2,3]

The use of zeolites for stabilizing highly reactive metal clusters[4,5] and ionic clusters, such as $Na_n^{(n-1)+}$ and $K_n^{(n-1)+}$,[6-21] has been of great recent interest. Exposure of zeolites with high-alumina contents to sodium metal vapor produces color centers which have been associated with ionic sodium clusters located in zeolite cages.[6-10] The properties of ionic clusters and studies on their formation have been of interest for synthetic and potential catalytic applications.[6-16] Absorption studies have also been investigated on Na_4^{3+} clusters in sodium sodalite materials.[22]

Ionic clusters have been reported to form in octahedral[12,14,20] or tetrahedral[13,16,23] geometries. The geometry of these highly charged clusters is unusual because of the existence of high charge density confined to a small area of the zeolite. The small zeolite cages and accompanying negatively charged framework make zeolites good host materials for highly charged ionic clusters. Ionic clusters are stabilized inside zeolite cages due to steric and electrostatic effects from the zeolite matrix. The "protective" framework of the zeolite enables spectroscopic and catalytic studies to be carried out on these highly unusual and reactive species.

There are few detailed studies on the catalytic activity of ionic clusters in zeolites.[11,16,17] Sodium ionic clusters, formed by the decomposition of sodium azide, have been studied in double-bond isomerization of *cis*-2-butene and in the hydrogenation of acetylene and benzene.[17] Ionic sodium clusters have been prepared by the decomposition of NaN_3[17-19] and by photoirradiation.[23,24] γ-irradiation of zeolites has been reported to create solid-state defect sites resulting in materials with altered catalytic activity.[25,26]

Metallic clusters formed in zeolites have been of interest for their catalytic properties in hydrogenation reactions and in reforming reactions.[4,5,27,28] Fe-Mn mixed-metal clusters in zeolites have been studied as CO hydrogenation catalysts.[4] Other small-particle bimetallic clusters of group VIII (Fe, Co, Ni) metals have also been prepared in zeolites.[5] Bimetallic cluster catalysts have been used in commercial reforming of petroleum fractions and in improving selectivities for a number of hydrocarbon reactions.[27,28] Small particle transition metal clusters formed in zeolites are highly stable in comparison to

* To whom correspondence should be sent.
[†] Department of Chemistry, University of Connecticut.
[‡] Texaco, Inc.
[§] Department of Chemical Engineering and Institute of Materials Science, University of Connecticut.
[⊗] Abstract published in *Advance ACS Abstracts*, March 1, 1995.

0022-3654/95/2099-4698$09.00/0

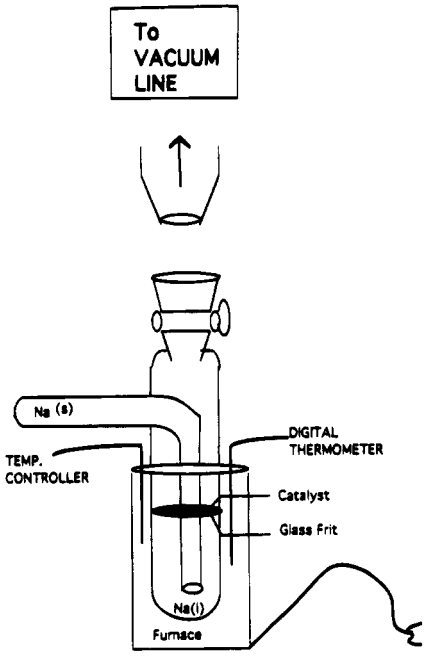

Figure 1. Chemical vapor deposition (CVD) reactor used in the application of sodium.

ionic clusters. Studies of the catalytic properties of ionic clusters, however, have been limited due to complicated synthetic procedures and their sensitivity to air and moisture.[16]

This work focuses on the characterization of NaX zeolites chemically treated with sodium vapor. Resulting materials are used in cyclopropane isomerization reactions. Catalytically active sites have been studied by magic angle spinning nuclear magnetic resonance (MAS NMR), electron paramagnetic resonance (EPR), and Fourier transform infrared spectroscopy (FTIR) methods. EPR experiments of sublimed naphthalene on these materials were carried out to illustrate the presence of catalytically active defect sites in these materials. Stability of such materials is also studied by spectroscopic techniques. Mechanisms for the formation and thermal decomposition of ionic clusters and defects are mentioned.

II. Experimental Section

A. *Synthetic Approaches. 1. Preparation of Sodium Ionic Clusters.* About 0.25 g of 60 mesh NaX zeolite (Linde, from Alfa Ventron, Danvers, MA) was thoroughly dehydrated in a quartz tube at 380 °C for 15 h under vacuum (1×10^{-4} Torr). Complete dehydration of these materials is imperative, because even trace amounts of water can effect product formation in the zeolite cages. The dehydrated sample was transferred into a drybox under an ultrahigh-purity N_2 atmosphere and loaded into a quartz reactor, hereafter called a chemical vapor deposition (CVD) reactor, shown in Figure 1. The CVD reactor, having a diameter of $^7/_8$ in., contains a drop tube outside of the furnace to hold the solid metal, an internal tube leading from the drop tube to the base of the reactor, a semipermeable glass frit to support the zeolite, and a 24/40 male adapter for connection to a vacuum line. Based on the formula for the unit cell of dehydrated NaX zeolite, $Na_{86}Al_{86}Si_{106}O_{384}$, about 1.2 wt % sodium was required to maximize the number of ionic clusters that could be formed in the zeolite. The amount of sodium used in these studies theoretically places one ionic cluster in each of the eight sodalite cages of each unit cell of the zeolite, assuming that one vaporized Na^0 atom leads to the formation of one ionic cluster. Taking this under consideration, an excess of sodium (about 25 mg) was added to the quartz tube in order to account for some loss of material in transfer and to compensate for any oxide species on the surface of the metal. The sodium metal was transferred into the drybox and added to the drop tube of the CVD reactor.

The CVD reactor was sealed off and transferred back to the vacuum line, and the catalyst was heated to 380 °C for 1 h to ensure complete dehydration. The temperature was reduced to room temperature, and the sodium was introduced into the bottom of the reactor. The temperature was slowly raised to 225 °C, and the metal was vaporized onto the zeolite. The temperature was held at 225 °C until nearly all the metal was vaporized and until the color of the zeolite turned from white to dark blue (approximately 10 min, depending on heating rate). The reactor was cooled and transferred back to the drybox where it was sealed and stored for characterization and catalytic studies.

2. Sublimation of Naphthalene. Following CVD of sodium vapor, a small quantity of the material was treated with naphthalene. Naphthalene was sublimed onto the zeolite using a quartz tube on a vacuum line. The tube consists of a side arm which holds the naphthalene and a straight portion which holds the sodium-modified zeolite. Materials were loaded into the sublimation tube inside a drybox. The walls of the sublimation tube were heated with heat tape in order to prevent the naphthalene from condensing on the walls of the tube. A tube furnace was used to heat the naphthalene, and a liquid nitrogen dewar was used to condense the naphthalene onto the zeolite. About 10 mg of naphthalene was used to react with 25 mg of sodium-treated zeolite.

After the sublimation tube was thoroughly evacuated, the vacuum valve was closed and the naphthalene heated to about 120 °C. Liquid N_2 was applied only to the portion of the tube containing the zeolite. The sublimation was continued until all the naphthalene had vaporized.

Naphthalene was sublimed on three variations of Na-modified materials: sodium-treated NaX, sodium-treated NaX which was heated to 380 °C under vacuum, and sodium-treated NaX which was heated to 380 °C in air. All materials contained the same amounts of sodium and naphthalene. The samples were brought into a drybox and sealed in quartz tubes for EPR analysis.

B. *Characterization. 1. Electron Paramagnetic Resonance.* Electron paramagnetic resonance (EPR) measurements were carried out on a Varian E-3 ESR spectrometer at room temperature and 77 K near a frequency of 9.0 and 9.1 GHz with 100 kHz magnetic field modulation and a modulation amplitude of 4.0 G.

2. Magnetic Angle Spinning Nuclear Magnetic Resonance (MAS NMR). MAS NMR experiments for ^1H, ^{23}Na, ^{27}Al, and ^{29}Si were done on a Varian Unity-300 superconducting NMR spectrometer system with full solids capacity. All spectra were acquired using a 7 mm, high-speed CP/MAS probe obtained from Doty Scientific, Inc. ^1H MAS spectra were acquired at 299.95 MHz using a single-pulse experiment at 7 kHz MAS speed, using a 10° pulse tip angle and a 0.5 s recycle delay. Background ^1H static spectra arising from probe materials were subtracted from all ^1H spectra. The ^{29}Si spectra were acquired at 59.59 MHz with a 4 kHz MAS speed, using a 30° pulse tip angle and a 5 s recycle delay. The ^1H and ^{29}Si spectra were referenced to tetramethylsilane (0 ppm). The ^{27}Al spectra were acquired at 78.16 MHz, with a 7 kHz MAS speed, a 10° pulse tip angle, and a 0.2 s recycle delay. ^{27}Al spectra were referenced to crystalline $KAl(SiO_4)_2 \cdot 18H_2O$ (0 ppm). ^{23}Na spectra were acquired at 79.35 MHz with a 5−7 kHz MAS speed, a 10° pulse tip angle, and a 0.5−1 s recycle delay. ^{23}Na spectra were referenced to solid NaCl (0 ppm). All ^{27}Al, ^{29}Si, and ^{23}Na spectra were acquired with a single-pulse experiment with high-

power decoupling. Zirconia MAS rotors with tight-fitting end caps were used with the Doty probe.

MAS NMR analyses were carried out on standard, untreated NaX zeolite, as well as samples of NaX treated with Na(v). The samples treated with Na(v) are the same as those studied by EPR and in catalytic reactions. Na(v)-treated samples were sealed in quartz tubes following the synthesis and loaded into the MAS NMR rotors under inert conditions in a glovebox to prevent exposure to air. The rotor end caps were tight fitting enough that no hydration of the sample occurred during the NMR experiment.

3. Fourier Transform Infrared Spectroscopy. FTIR spectra were collected on a Nicolet spectrometer with 2 cm^{-1} resolution by using a deuterated triglycerine sulfate (DTGS) KBr detector. NaX zeolites treated with Na vapor were studied via infrared before and after exposure to air and before and after thermal treatment at 380 °C by using 15 mg (neat) pellets. Framework vibrations and acidity of NaX were also studied by infrared analysis. Brønsted and Lewis acidities of both Na-treated and untreated NaX zeolite were determined by quantitatively measuring chemisorbed pyridine in a manner previously described.[29]

4. Luminescence. Zeolites exposed to sodium vpaor were sealed in an evacuated 2 mm diameter quartz tube for luminescence analysis. Luminescence excitation and emission spectra were recorded with a Spex Model 1680B 0.22 m double-monochromator luminescence spectrophotometer. An Osram XBO 450 W xenon arc lamp was used for excitation.

5. X-ray Powder Diffraction. X-ray powder diffraction (XRD) experiments were done on a Scintag Model PDS 2000 diffractometer. Samples were mounted on glass slides by sprinkling powder on the slides to avoid preferential ordering. A beam voltage of 45 kV and a current of 40 mA were used. Samples were scanned from 5° to 60° 2θ.

C. *Catalysis.* In a drybox, 150 mg of NaX treated with Na vapor was loaded into a stainless steel reactor having a length of 12 in and an i.d. of 5 mm. The catalyst was supported on a 200 mesh stainless steel screen and glass wool. The sample was treated in He (20 cm^3/min) at 380 °C. A diagram of the reactor system showing the gas feed system, reactor, gas sampling valve, gas chromatograph, flow meters, and bubble meters can be found elsewhere.[29]

A thermal conductivity detector (TCD) was used on a 5580A Hewlett-Packard gas chromatograph with Poropak Q and T columns in series. The gas sampling system and calibration methods can be found elsewhere.[29]

The partial pressure of reactant was held constant by using a 1:10 mixture (9.09 mol %) of cyclopropane (c-C_3H_6) in He in all experiments. Temperature was varied from 220 to 380 °C in order to determine apparent activation energies of reaction by using the Arrhenium equation as shown in eq 1,

$$\ln k = \ln(A) - (E_a/R)(1/T) \quad (1)$$

where A is the preexponential factor, E_a is the apparent activation energy, R is the ideal gas constant (82.057 cm^3 atm/(mol K)), and T is the reaction temperature in kelvin.

Rates of propylene formation were derived based on the following:

$$\text{rate} = (PQ_0/RT_0)p_{C_3H_6}/W \quad (2)$$

where P is the total pressure (1 atm), Q_0 is flow rate in mL/s (ambient), T_0 is the temperature (298 K), $p_{C_3H_6}$ is the partial pressure of propylene leaving the reactor, and W is weight of the catalyst(g). Rates of C_3H_6 formation are expressed as mol/(s g).

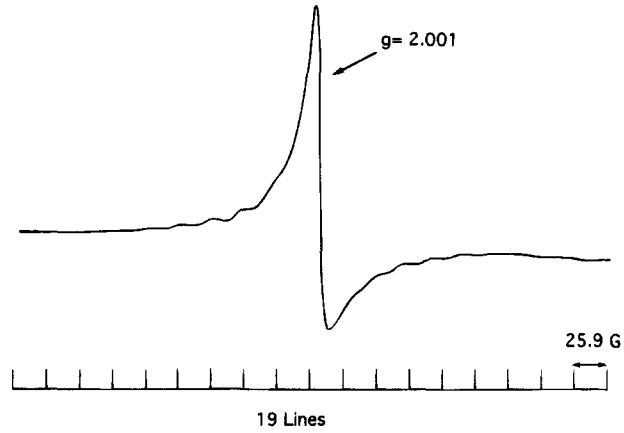

Figure 2. EPR spectrum of Na(v)/NaX zeolite at 77 K; scanned at a magnetic field, H, of 3250 ± 250 G, with a ν of 9.13 GHz.

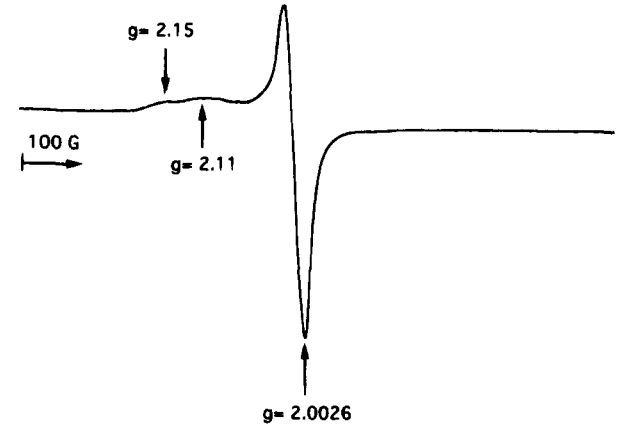

Figure 3. EPR spectrum at 77 K; scanned at a magnetic field, H, of 3300 ± 500 G and a ν of 9.13 GHz for Na(v)/NaX exposed to air.

A 20% mixture of 1-butene (1-C_4H_8) in Ar was prepared and studied in isomerization reactions over Na(v)/NaX materials. This analysis was carried out in a manner similar to c-C_3H_6 isomerization reactions. Catalytic studies using 1-butene were carried out from room temperature to 100 °C.

III. Results

A. *Characterization. 1. EPR.* The EPR spectrum of Na(v)/NaX, as prepared, is shown in Figure 2. This spectrum was taken at 77 K with a scan range of 3250 ± 250 G and with a receiver gain of 2.5 × 10^2. The sharp band at H = 3247.5 G has a corresponding g value of 2.001. A total of 19 smaller lines can be recognized between 3000 and 3500 G. The outer six lines of this spectrum are very weak in intensity and can be observed only upon expanding the spectrum off-scale. In addition, three of these lines are convoluted underneath the intense peak centered at 3247.5 G. This was confirmed by measuring a hyperfine splitting constant (A value) of 25.9 G.

EPR spectra collected on Na(v)/NaX samples exposed to air did not show hyperfine splitting, but instead showed three peaks located at g = 2.0026, 2.0083, and 2.0780. This spectrum is shown in Figure 3 at a scan range of 3300 ± 500 G. Upon heating this material to 380 °C, the EPR spectrum (Figure 4) shows a single intense peak at a g value of 2.0026. Two smaller, broad bands are observed at lower magnetic field. The g values of these bands are between 2.11 and 2.15. The hyperfine splitting structure of this material disappears upon heating at elevated temperatures.

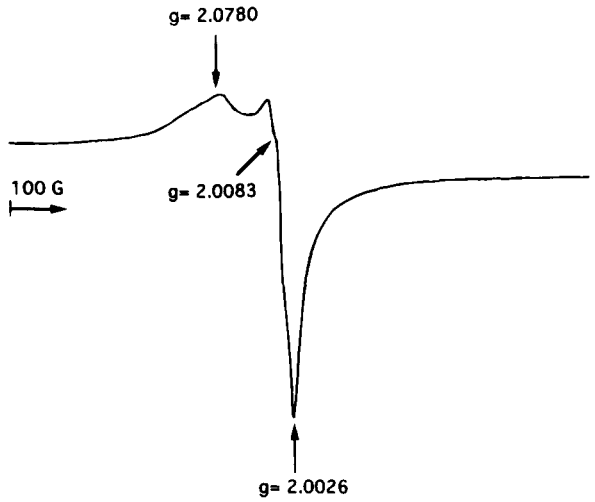

Figure 4. EPR spectrum at 77 K; scanned at a magnetic field, H, of 3300 ± 500 G and a ν of 9.13 GHz for Na(v)/NaX heated to 380 °C.

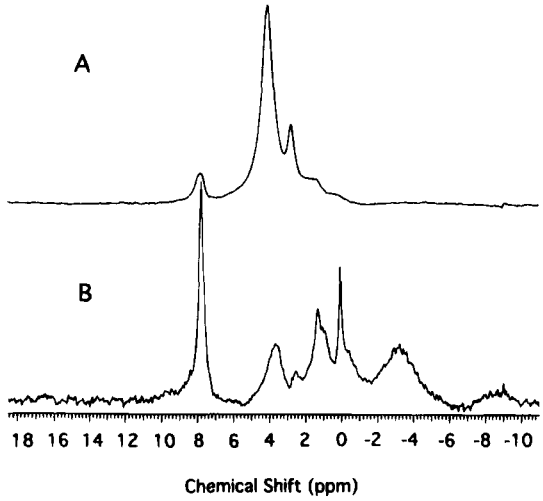

Figure 5. ^{1}H MAS NMR spectra of (A) dehydrated NaX and (B) Na(v)/NaX zeolite.

Samples prepared with excess sodium showed a single sharp peak having a g value of 2.0013. The EPR spectrum of this material (not shown) reveals little evidence of hyperfine splitting.

2. ^{1}H, ^{23}Na, ^{27}Al, and ^{29}Si MAS NMR. ^{1}H MAS NMR spectra for NaX and Na(v)/NaX are shown in Figure 5. In the untreated NaX zeolite, shown in Figure 5a, typical surface hydroxyl resonances (Si−OH) of NaX are observed at 1.8 ppm, Al−OH resonances are observed at 2−3 ppm, and bridging hydroxyl groups (Al−O(H)−Si) are apparent between 3 and 6 ppm. A signal of weaker intensity is observed at 7.8 ppm. The spectrum of Figure 5b, corresponding to Na(v)/NaX zeolite, shows a dramatic decrease in the ^{1}H signal intensity of the Al−O(H)−Si, Al−OH, and Si−OH resonances between 0 and 6 ppm. Surface hydroxyl groups at 1.8 ppm still present in Na(v)/NaX materials, however, are significantly reduced in concentration. A single, sharp signal is observed at approximately 0 ppm. A significant resonance is observed at −3 ppm. The resonance at 7.8 ppm in both materials is about the same order of intensity. The data of Figure 5 were plotted to full scale for each analysis; however, the difference in the two signals is that the intensity of the resonance of 7.8 ppm is much greater relative to the total hydroxyl contribution in sodium vapor-treated materials. The overall intensity of all hydroxyl groups in Na(v)/NaX materials has significantly decreased. This indicates that the species at 7.8 ppm may not be accessible to Na vapor, while hydroxyl groups are effected by sodium vapor. These

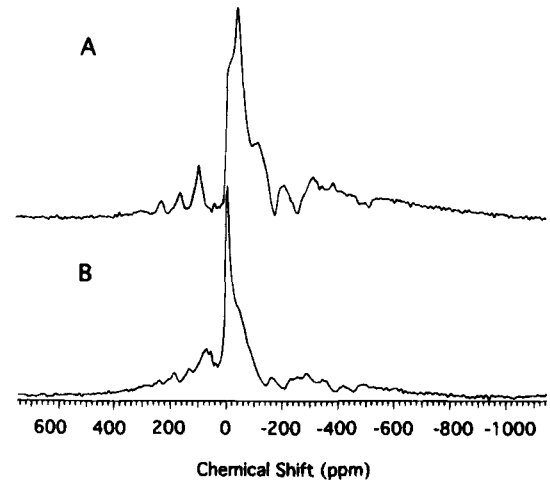

Figure 6. ^{23}Na MAS NMR spectra of (A) dehydrated NaX and (B) Na(v)/NaX zeolite.

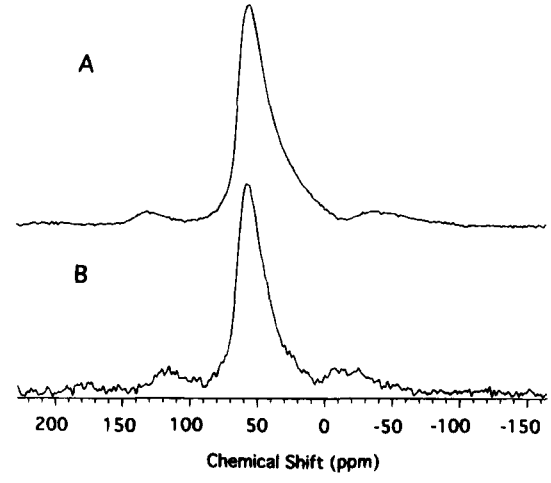

Figure 7. ^{27}Al MAS NMR spectra of (A) dehydrated NaX and (B) Na(v)/NaX zeolite.

data strongly suggest that sodium vapor is highly reactive with hydroxyl groups of the zeolite.

^{23}Na MAS NMR spectra for NaX and Na(v)/NaX are shown in Figure 6. The ^{23}Na MAS NMR spectrum for NaX zeolite, shown in Figure 6a, reveals a broad asymmetric resonance due to several types of Na which are located between 0 and −150 ppm. This signal is surrounded by intensity due to spinning sidebands. Variable spinning speed experiments reveal the presence of at least four types of sodium contributing to the line shape. Broad resonances were also observed in samples heated at 380 °C (spectrum not shown). The ^{23}Na NMR spectrum of Na(v)/NaX (Figure 6b) shows a much sharper, more symmetric signal with the majority of intensity at −12 ppm.

^{27}Al MAS NMR spectra of NaX and Na(v)/NaX are shown in Figure 7. Figure 7a shows the ^{27}Al NMR spectrum for NaX zeolites. This spectrum has a single, relatively broad peak located at 65 ppm. This peak is indicative of tetrahedral Al located in the framework of the zeolite. Figure 7b shows a similar signal which also corresponds to tetrahedral aluminum. The similarity in the line shapes of these two samples will be discussed.

The ^{29}Si MAS NMR spectrum for NaX zeolite (Figure 8a) depicts four signals which are consistent with various Si sites typical of NaX zeolites. The Si:Al ratio of this material is about 1.25. The ^{29}Si NMR for Na(v)-treated NaX is shown in Figure 8b. This spectrum reveals similar framework assignments for silicon between −80 and −110 ppm. The Si:Al ratio is about

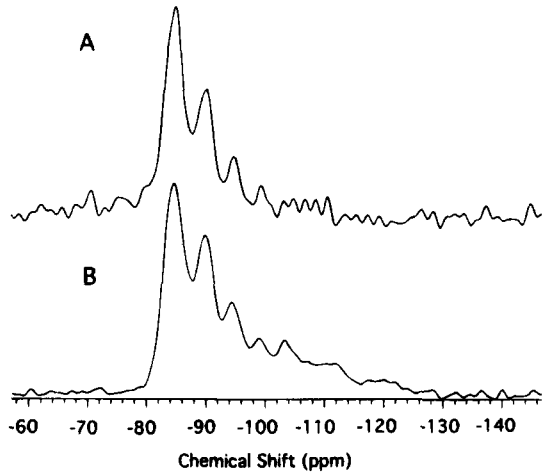

Figure 8. ^{29}Si MAS NMR spectra of (A) dehydrated NaX and (B) Na(v)/NaX zeolite.

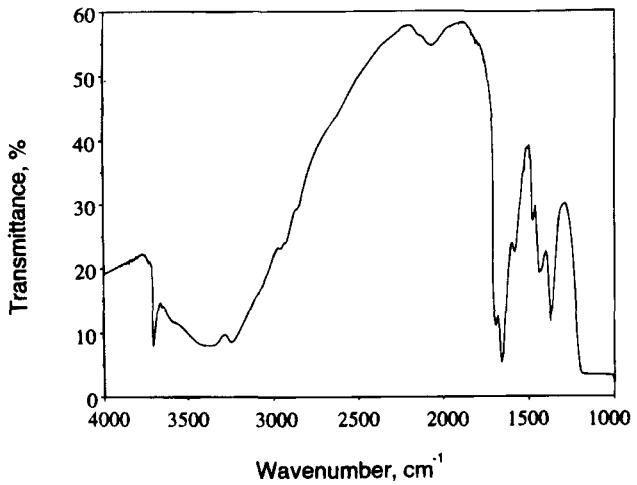

Figure 9. *Fourier transform infrared spectrum of Na(v)/NaX treated with pyridine for 1 h at room temperature.*

1.4. This suggests that slight dealumination has occurred in materials treated with sodium vapor.

3. FTIR Data. The FTIR spectrum of Figure 9 corresponds to the analysis of adsorbed pyridine on materials containing sodium ionic clusters. The presence of a vibrational band at 3695 cm^{-1} is observed in all sodium-modified zeolites that were not exposed to air or heat. This band is not observed in unmodified NaX zeolites. A broad band centered at 2000 cm^{-1} is also observed. The spectrum of Figure 9 also shows a broad band between 3550 and 3000 cm^{-1} which is indicative of the presence of water in this material. Water contamination is likely to have occurred upon transfer of the sample pellet into the infrared cell.

The bands of Figure 9 at 1690, 1650, 1590, 1490, 1460, and 1365 cm^{-1} correspond to physisorbed pyridine or Si−O or Al−O vibrational bands, indicating some deformation of the zeolite framework. The band at 1460 cm^{-1} corresponds to Lewis acidity. Adsorption of pyridine on acid sites in unmodified NaX zeolite results in a very weak adsorption band at 1541 cm^{-1}, consistent with Brønsted acidity, and a stronger band at 1460 cm^{-1}, consistent with Lewis acidity. The FTIR spectrum of Na(v)/NaX materials (Figure 9) does not show any transmittance band at 1540 cm^{-1}, suggesting that loss of Brønsted acidity occurs when NaX is treated with sodium vapor. The band at 1460 cm^{-1} was observed to increase upon CVD treatments with sodium.

The infrared spectrum of Na(v)/NaX heated to 380 °C is shown in Figure 10 from 4000 to 1800 cm^{-1}. This spectrum

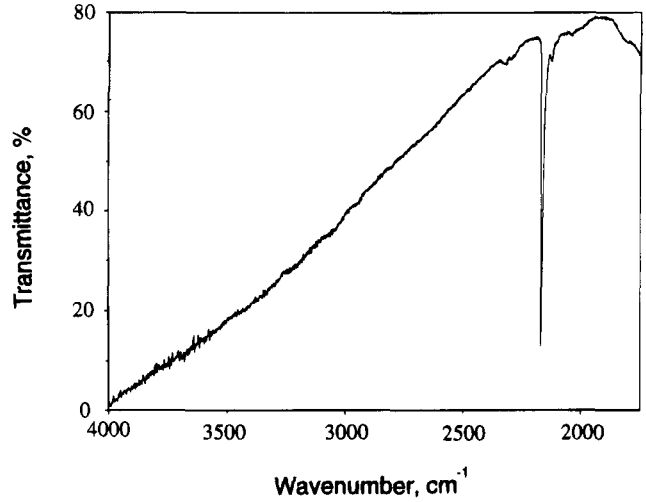

Figure 10. FTIR spectrum of Na(v)/NaX heated to 380 °C plotted from 4000 to 1800 cm^{-1}.

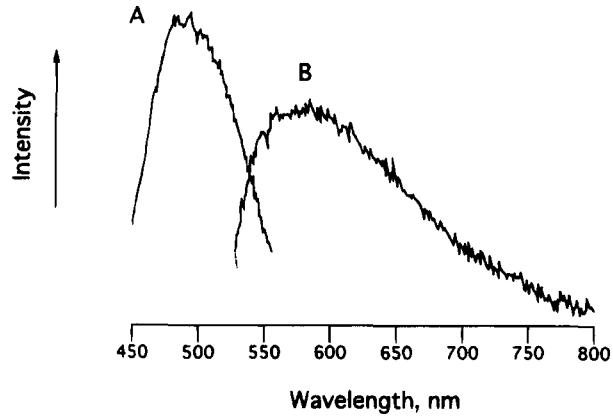

Figure 11. Luminescence excitation and emission spectra of Na(v)/NaX: (A) λ_{ex} = 475 nm, (B) λ_{em} = 575 nm.

reveals an extremely intense band at 2208 cm^{-1}. This band is, in most cases, the strongest observed in the spectrum and, to our knowledge, has never been observed in zeolites. This material shows no evidence of hydroxyl groups, indicative of either Brønsted acidity or water.

4. Luminescence. The luminescence excitation and emission spectra of Na(v)/NaX are shown in Figure 11. This sample shows an excitation maximum, having a relatively strong intensity of 6 × 10^4 counts per second (cps), for a species at a wavelength of 475 nm. An emission band corresponding to this excitation is observed at a wavelength of 575 nm. Untreated NaX zeolite was also analyzed by luminescence in the range 300−800 nm, and no excitation or emission bands were observed.

5. XRD. X-ray diffraction patterns were obtained for both NaX and Na(v)/NaX zeolites. A slight decrease in peak intensities was observed in the Na(v)/NaX zeolite, which had been exposed to air during analysis. Additional peaks corresponding to oxide species or sodium metal were not observed in the diffraction patterns of sodium-treated materials. This suggests that crystalline Na or Na_2O is not present in sodium-modified materials or that particle sizes are smaller than 50 Å. Na(v)/NaX samples heated to 380 °C show a decrease in overall intensity, but the relative intensity of all peaks appears to be the same.

B. *Catalysis.* Results of c-C_3H_6 isomerization experiments are shown in Figure 12. These plots show the percent conversion and rates of propylene formation (mol/(s g) × 10^6)

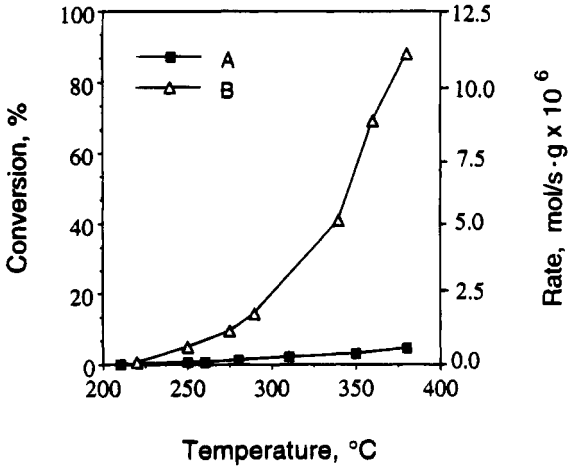

Figure 12. c-C_3H_6 conversion (%) and rate of propylene formation (mol/(s g)) × 10^6 as a function of temperature for (A) NaX and (B) Na(v)/NaX zeolite.

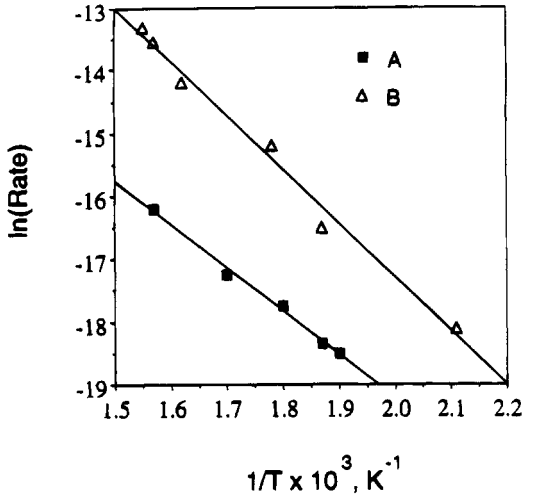

Figure 13. Arrhenius plot of ln(rate) of C_3H_6 formation *vs* $1/T \times 10^3$ $(K)^{-1}$ for (A) NaX and (B) Na(v)/NaX.

as a function of reaction temperature (°C) for both NaX and Na(v)/NaX. At 220 °C, both NaX and Na(v)/NaX have very low catalytic activities with conversions less than 1%. At 320 °C, however, Na(v)/NaX begins to show significant activity. An almost linear increase in reaction rate with increasing temperature is evident up to 380 °C, where nearly 90% conversion is observed. NaX zeolite, on the other hand, shows negligible activity (<5% conversion) at 380 °C. The low activity of NaX can be attributed to trace amounts of Brønsted acidity initially present in the zeolite. In addition, the activity of Na(v)/NaX increases with increasing time on stream, while the activity of NaX zeolite has been known to decrease with increasing reaction times.[29]

Figure 13 shows an Arrhenius plot of $(1/T) \times 10^3$ K^{-1} vs ln(rate) where the slope of the line is equal to $-E_a/R$. From this plot, apparent energies of activation (E_a) for cyclopropane isomerization reactions over NaX and Na(v)/NaX are obtained. NaX has an E_a of 13.5 kcal/mol while Na(v)/NaX has a higher E_a of 16.4 kcal/mol.

1-Butene reactions studied over Na(v)/NaX materials showed no evidence of isomerization to 2-butene at room temperature. Even at 100 °C a cis/trans ratio of 2-butene greater than the thermodynamic equilibrium value of approximately 1:2 was not observed.

C. *Naphthalene Sublimation.* Figure 14 shows EPR spectra of naphthalene sublimed onto Na(v)/NaX zeolite. The spectrum

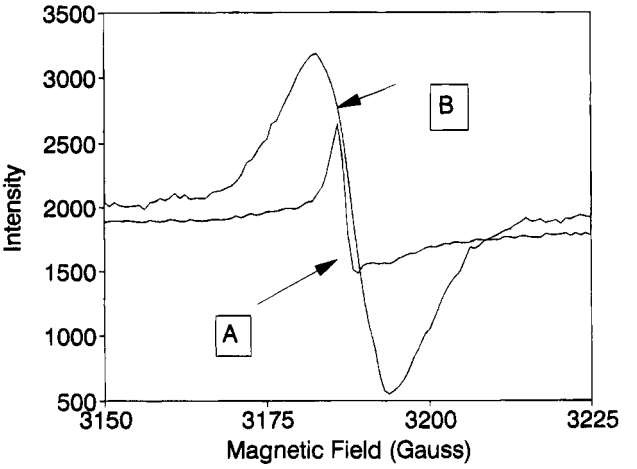

Figure 14. EPR spectra at 100 K of sublimed naphthalene on (A) Na(v)/NaX zeolite as prepared and (B) Na(v)/NaX heated to 380 °C under vacuum. Magnetic field scan range is 3187.5 ± 37.5 G, with a ν of 8.95 GHz.

shown in Figure 14a corresponds to naphthalene sublimed onto Na(v)/NaX zeolite, as prepared. Figure 14b shows the EPR spectrum of naphthalene sublimed onto Na(v)/NaX zeolite which was heated under vacuum to 380 °C. Figure 14a reveals a single sharp peak centered at a g value of 2.0112. This spectrum does not show any splitting pattern which might be due to a naphthalene cation radical. Splitting due to the sodium ionic clusters has also been significantly reduced.

Upon heating these materials the EPR spectrum (Figure 14b) shows a shift to a lower g value of 2.003. The shift to lower g values upon heating is consistent with EPR measurements taken on freshly prepared samples not containing naphthalene. The spectrum of naphthalene sublimed onto heated Na(v)/NaX samples shows peak broadening of the central peak and significant intensity due to hyperfine splitting.

IV. Discussion

A. *Sodium Ionic Clusters.* Upon exposure to Na vapor at 225 °C for about 10 min, the dehydrated NaX zeolite turned from white to light blue and finally to dark blue or purple in color. Blue or purple color centers for NaX zeolites exposed to Na^0 vapor have been previously reported.[12-14,20] Others report pink color centers for NaY zeolites exposed to Na vapor or NaN_3.[6,7,11,16,30] Pink color centers have been associated with Na_4^{3+} ionic clusters, while blue color centers are observed with Na_6^{5+} clusters. Upon exposure to air, these samples immediately turned pale yellow or off-white in color. This is consistent with previous literature reports.[10,13,16] Samples treated with sodium for longer periods of time, i.e., samples having high concentrations of sodium, were black or gray in color, consistent with previous reports.[10,12,15] These samples exhibit little or no hyperfine splitting structure found in ionic clusters. When samples with high sodium concentrations are exposed to air, the black color faded over a period of several hours and remained gray in color. The gray color and slow diffusion rates of oxygen suggest that sodium metal clusters or particles are formed and block zeolite pores when excess sodium is used. The use of excess metal in the CVD of sodium was avoided for catalytic and spectroscopic analyses. Atomic absorption analysis shows a total sodium weight percent of 11.4%, which is equivalent to an excess of 1.2 wt % sodium added to the zeolite. From elemental analysis data, the net unit cell composition for sodium-treated NaX zeolite was determined to be $(Na^0)_{10}(Na^+)_{86}Al_{86}Si_{106}O_{384}$.

TABLE 1: Literature Data on g Values and Hyperfine Splitting Constants for Various Sodium Ionic Clusters in NaX and NaY Zeolites

sodium ionic cluster	zeolite	color and no. of lines	g value (lit.)	A value (G)	ref
Na_4^{3+}	NaX	purple/13	2.0002	29.0	13
Na_4^{3+}	NaX	purple/13	1.9990	28	23
Na_4^{3+}	NaY	red/13	2.0012	32.5	30
Na_4^{3+}	NaY	pink/13	2.0012	32.5	7
Na_5^{4+}	NaX	blue/16	*a*	*a*	14b
Na_6^{5+}	NaX	dark blue/19	2.0013	25.9	12
Na_6^{5+}	NaX	blue/19	2.001	27	20
Na_6^{5+}	NaX	purple/19	2.0022	25.0	14b
Na_6^{5+}	NaX	purple/19	2.001	25.9	this work

[a] Not reported.

B. *Spectroscopic Techniques. 1. EPR.* The intense asymmetric center line at $g = 2.001$ in the EPR spectrum for sodium ionic clusters has been assigned to small sodium particles in the cages of NaX,[10] as pointed out by a reviewer. This is consistent with previous assignments for Na metallic particles and bulk metal which have been reported to have g values of 2.0013 and 2.0015, respectively.[31,32] The band at $g = 2.001$ overlaps three other peaks as well as the central line splitting of the cluster itself. The g value of 2.001 and the hyperfine splitting constant of 25.9 G are both consistent with Na_6^{5+} ionic clusters reported for sodium-treated NaX zeolites.[12,20,30] Table 1 shows a summary of g values and hyperfine splitting constants reported for various sodium ionic clusters in NaX and NaY zeolites.

A total of 19 lines is expected to be observed for Na_6^{5+} ionic clusters due to the contribution of six Na^+ ions in an octahedral arrangement. This observation is based on the $(2nI + 1)$ rule with $I^{23}_{Na} = {}^3/_2$ and $n = 6$ for each sodium ion in the cluster. In the EPR spectrum shown here, the central 13 lines are clearly observed; however, the outer six lines are extremely weak in intensity but are still present in these materials. In cases of low concentrations of Na^{65+} ionic clusters, the intensity of the outer hyperfine splitting lines may not be within the detection limits of the instrument. In our EPR analyses, spectra for ionic clusters were expanded off-scale in order to detect the weaker, outer lines of the spectrum. An A value of 25.9 G results in 19 bands within a 492 G range.

An octahedral environment is the most stable, least strained, and lowest energy arrangement of Na^+ ions in the sodalite cages of the zeolite.[22] Ionic clusters are believed to form from cationic sodium ions present in the zeolite, as shown in eq 3. The electron supplied to the cluster is believed to originate from the oxidation of sodium metal. These observations and the generalized equation expressed in (3) are consistent with previous reports.[10]

$$6Na^+ + Na^0 \rightarrow Na_6^{5+} + Na^+ \qquad (3)$$

The color center associated with the ionic clusters and a g value near that of a free electron ($g = 2.0023$) suggest that a highly energetic and localized unpaired electron is associated with the octahedra of sodium ions. The unpaired electron in Na_6^{5+} clusters reported by Kevan et al. has been found to interact equally with all ^{27}Al nuclei in the sodalite cage (β-cage), as determined by Fourier transform electron spin echo modulation (FT-ESEM) experiments.[30] The constrained environment of the sodalite cage and the high negative charge associated with the zeolite framework of NaX is likely to stabilize these highly energetic species.

Samples of NaX exposed to excess sodium resulted in black materials having an EPR spectrum with a g value of 2.0013. This is consistent with Na^0 particles greater than 1000 Å in size.[31] Hyperfine splitting, indicative of ionic clusters, was not observed in these materials. This is consistent with studies by Anderson et al., who reported that the loss of hyperfine splitting in zeolites containing high concentrations of Na^0 could be attributed to interactions between two or more ionic clusters within 12 Å of each other.[33] Sodium ions of clusters in adjacent sodalite cages are approximately 5 Å apart. This is based on geometric calculations on the clusters and the free pore diameter of the zeolite. Electron hopping between ionic clusters of adjacent sodalite cages has also been suggested.[33]

An additional reaction that occurs when NaX zeolites are exposed to sodium vapor is represented by eq 4. This mechanism accounts for the loss of Brøsted acidity as a result of treatment with sodium vapor and implies that there is a 1:1 stoichiometry between Brønsted sites ($H^+_{zeolite}$) and ionic clusters. This mechanism shows that resultant electron holes (h^+) are present in sodium-treated materials. These holes result from the donation of an electron from framework oxygen of the zeolite to the Na_6^{5+} cluster, which, in turn, stabilizes the highly charged complex in the sodalite cage of the zeolite. A g value of 2.0123 has previously been assigned to holes in NH_4Y and HY zeolites.[24,34] The loss of Brønsted acidity may result in the generation of hydrogen radicals as shown in the redox reaction of eq 4; or proton loss may occur in the form of

$$5Na^+ + H^+_{zeolite} \xrightarrow{Na^0} Na_6^{5+} + h^+ + H^\bullet \qquad (4)$$

molecular hydrogen. We have no evidence for the generation of H_2 during the reduction of Brønsted acidity. Further, the amount of Brønsted acidity present in these materials is very low; therefore, the production of H_2 or atomic hydrogen will be limited. Although the presence of Brønsted acidity is conceivably not necessary for ionic cluster formation, the mechanism of eq 4 justifies the loss of Brønsted acidity during reaction with sodium vapor. It has been suggested by a reviewer that the generation of electron holes may very well be a result of direct reaction between surface hydroxyl groups and sodium metal and may not involve cluster formation at all. The production of atomic hydrogen and the reduction of Brønsted acidity are consistent with FTIR and pyridine chemisorption experiments which will be discussed later.

The EPR spectrum of ionic clusters exposed to air shows an intense signal at $g = 2.0026$, a shoulder at $g = 2.0083$, and a weaker signal at $g = 2.0780$, which are consistent with oxygen radicals. Specifically, the data of Figure 3 suggest that the superoxide anion, O_2^-, is the EPR-active species in these materials. This is consistent with previous reports.[34,35] Irradiated zeolites exposed to air at room temperature also show three **g** tensors in the EPR spectrum taken at 77 K.[34] These g values, $g_{xx} = 2.0026$, $g_{yy} = 2.0085$, and $g_{zz} = 2.0575$, have been observed in NH_4Y zeolites.[34] In NaX zeolites, $g_{zz} = 2.078$ has been assigned to a O_2^- superoxide species adsorbed on Na^+.[35] The absence of hyperfine structure in this sample suggests that there is no interaction between O_2^- and electron holes associated with aluminum.[34]

The data of Figure 4 show a loss of fine structure and a slight shift in g values upon heating at 380 °C, which suggests that the decomposition of ionic clusters occurs at high temperatures. This is consistent with previous reports.[6,23] The EPR spectrum obtained for this material is very similar to those reported for the superoxide anion attached to a nearby Na^+ cation.[6,35] The decay of the band at $g_{zz} = 2.078$ into a broad band containing

TABLE 2: Experimental and Literature Data of g Values for Sodium-Treated Materials

sodium treatment	color	g value (exptl)	g value (lit.)	assignt	ref
low sodium loading	purple	2.001	2.001	ionic clusters	20, 33
low sodium loading	off-white	2.0026	2.0016	surface O_2^-	35
		2.0083	2.0066		
exposed to air		2.0078	2.0078	defect site on framework O	6
low sodium loading	white	2.0026	2.003	O_2^-–Na^+	36, 37
heated at 380 °C in air		2.11–2.15	2.113	surface O_2^-	35
excess sodium loading	gray/black	2.0013	2.0013	Na particles	31
			2.0015	bulk Na metal	32

several new components between g_{zz} = 2.11 and 2.15 is consistent with a previous study for samples irradiated at 77 K that were warmed.[36] Broadening of the g_{zz} component is also likely to occur in these systems due to strong dipolar interactions when atomic hydrogen combines with O_2^-.[36] The generation of atomic hydrogen in these systems and its consequences will be discussed later in more detail. The sharp band at g = 2.0026 may also correspond to a surface defect site, which has been reported to have a value of 2.003.[37] Differences in EPR spectra between freshly prepared materials at 225 °C and materials heated to 380 °C suggest that the types of defect site present following heating are quite different from holes generated in the formation of the sodium ionic clusters. Heating of these materials is likely to change the environment surrounding defect sites and may cause migration of holes from one site to another.

The formation of O_2^- species can be attributed to the thermal breakdown of the Na_6^{5+} clusters. The source of oxygen is likely to be from the release of strongly adsorbed oxygen from the zeolite which is known to be released at high temperatures.[38] Thermal treatment results in greater interactions between trapped electrons and surrounding nuclei,[33] which might release trapped electrons. The decomposition of ionic clusters at high temperatures results in the release of the unpaired electron, which was once associated with the cluster. The electron is then trapped by gas phase oxygen molecules (trapped in the zeolite), which serve as an electron sink. It might be expected that electrons would quickly recombine with positive centered holes; however, it is well-known that cations adsorb O_2 molecules, and these species serve as excellent electron traps, giving rise to EPR signals characteristic of the superoxide ion.[6,35] This process suggests that active defect hole sites are produced after decomposition of Na_6^{5+} clusters. Table 2 shows a summary of experimental g values for modified Na(v)/NaX materials along with assignments and literature values.

We have studied the reaction of naphthalene with ionic clusters and holes by means of EPR. Naphthalene was chosen as a probe molecule for defect sites due to the distinct hyperfine splitting structure of the naphthalene radical. The data of Figure 14a show no evidence of peak broadening between 3175 and 3225 G that would result from the hyperfine splitting contribution of a naphthalene radical species. This suggests that radical cations are not formed in freshly prepared ionic cluster materials and that the ionic clusters themselves are not reactive toward naphthalene. The EPR spectrum of Figure 14b, however, is quite similar to that of the naphthalene cation radical. This radical cation shows peak broadening as in Figure 14b, which is about 34 G. The hyperfine splitting of this sample has an A value of 1.4 G, also consistent with the naphthalene radical. The g value of the naphthalene cation is also near 2.00. Both peak broadening and fine structure observed in Figure 14b are presumably the result of oxidation of naphthalene over positively charged defect sites on these materials as shown in eq 5.

$$C_{10}H_8 + h^+ \rightarrow C_{10}H_8^+ \quad (5)$$

Positive holes on oxygen atoms have been previously investigated using 3,3-dimethyl-1-butene as a probe molecule in EPR studies.[39] Solid state defect sites near g = 2.003 have been found to readily produce the 3,3-dimethyl-1-butene radical cation in ZSM-5 zeolites.[39] Radical cations prepared at low temperatures over defect sites, however, are usually limited to organic molecules with an ionization energy less than 9.0 eV.[40] Naphthalene has an ionization energy of 8.14 eV.[41] Intramolecular rearrangement reactions and reactions which generate carbenium ions are known to occur over positive holes.[42] The generation of hexamethylbenzene radical cations over positively charged holes has also been studied by EPR.[43] The reaction of aromatics and alkenes over positively charged defect sites and V-centers is well-known.[39,42,43]

These EPR data suggest that Na(v)/NaX materials heated to 380 °C are reactive toward naphthalene while those materials not thermally activated are unreactive toward naphthalene. These observations suggest that positively charged defect sites exist in these materials in order to maintain charge neutrality; however, the type of defect site or its surrounding environment is different than that of holes produced during cluster formation. This is consistent with EPR measurements taken on freshly modified zeolites which show a remarkable difference in EPR signals before and after heating. FTIR data also show a significant difference in spectra taken before and after heating Na(v)/NaX materials. There are far less adsorbed water species after heating Na(v)/NaX (Figure 10) than before heating (Figure 9). Electron holes may tend to increase the amounts of adsorbed water prior to heating.

Heating of some Na(v)/NaX materials may lead to sintering of Na^0 particles into $(Na)_x$ sodium agglomerates.[10,13] EPR and XRD results for our materials with low levels of sodium do not show this trend. The presence of oxygen in these materials is likely to result in oxidation of sodium metal upon decomposition of the ionic clusters, particularly at high temperatures. However, samples containing high levels of sodium (samples black in color) show evidence of particle migration and agglomeration from EPR data, giving rise to an intense signal for Na metal at g = 2.0013, consistent with agglomerates sodium.[28]

2. MAS NMR. The ^1H MAS NMR spectra of Figure 5 show significant differences for NaX zeolite and NaX treated with sodium vapor. The peak at 7.8 ppm can be attributed to a nonbonded hydronium ion as previously assigned[44] or to strongly adsorbed water on Lewis sites in the zeolite, which has been assigned a chemical shift of 6.5 ppm.[45] The nature of this Lewis site may effect its chemical shift values. The intensity of the resonance at 7.8 ppm remains strong, indicating that it is a site not effected by sodium vapor. The sharpening of this resonance following treatment with sodium vapor suggests that either sodium vapor selectively reacts with hydroxyl sites but not with the site at 7.8 ppm or that a completely new type of site is formed at 7.8 ppm as a result of sodium vapor treatment. The peak at 0 ppm or the broader resonances at −3 ppm can be attributed to hydridic species in the zeolite. These resonances are in the hydride chemical shift range; however, there are no previous reports for assignments of hydridic species in zeolites. A sharp decrease in Si−O(H)−

Al signals and a significant decrease in Si−OH and Al−OH resonances upon treatment with Na vapor is strong evidence that the reactive species with Na^0 are bridging and terminal hydroxyl groups. Redox reactions of Brønsted acid sites with Na vapor are well-known.[29]

The four components in the ^{23}Na NMR line shape of NaX (Figure 6a) correspond to Na^+ located at various sites (I, I′, III, and III) throughout the NaX zeolite framework. Most Na^+ ions reside in site I and I′ in the sodalite cages, while smaller amounts of Na^+ ions are located in the supercages. In NaX zeolite one observes signal intensity due to Na^+ in site I (hexagonal prism site) which gives rise to intensity at −12 ppm. The broader resonances in the −20 to −50 ppm region are due to a convolution of resonances from Na^+ in low symmetry sites II, III, and I′.[46,47] In this particular sample the broader line shapes are due to asymmetric II, III, and I′ sites for Na^+ that dominate the spectrum.

In the case of the Na(v)/NaX sample, one does not observe the same Na^+ distribution. The dominant feature of the spectrum (Figure 6b) is due to Na^+ in hexagonal prism sites. This resonance is narrow owing to the highly symmetric octahedral environment of the Na^+ ions. A dramatic loss of signal intensity after Na(v) treatment is observed in the −20 to −50 ppm range. This loss of signal intensity can be attributed to the presence of Na_6^{5+} clusters with trapped electrons within 10 Å of the Na^+ ions that are present in the asymmetric I′, II, and III sites. Thus, it appears that the Na_6^{5+} cluster is present in close proximity to only five of the six Na^+ sites in the zeolites. Finally, metallic Na^0 is not observed in the ^{23}Na spectra of the Na(v)-modified zeolites. This may be an indication that Na^0 is also closely associated with the Na_6^{5+} clusters which quench the NMR signals due to electron−nuclear dipole interactions.

^{27}Al NMR shows the presence of only framework tetrahedral aluminum, with no observation of extraframework aluminum. However, ^{29}Si NMR reveals a slight dealumination of the NaX zeolite by the sodium vapor modification. The ^{29}Si results do not reveal the presence of unusual surface Si species; however, this may be due to a low concentration of these species, preventing observation of these species at the signal-to-noise levels of these experiments.

3. FTIR. Infrared analyses of chemisorbed pyridine indicate that some initial Brønsted acidity is present in NaX zeolites. Infrared studies on Na(v)/NaX zeolites clearly show that Brønsted acidity is eliminated upon treatment with Na vapor, as illustrated in eq 4. This is consistent with earlier work on ion-exchanged Eu^{3+}/NaX, which showed that high initial Brønsted acidities were eliminated when exposed to sodium vapor.[29] EPR data for Eu^{3+}/NaX exposed to Na vapor show a reduction of Eu^{3+} ions to Eu^{2+}.[48] This is significant because it suggests that sodium vapor destroys the $(Eu_4O)^{10+}$ complex, which has been reported to form in the sodalite cages of NaX upon dehydration.[29,49]

Lewis acidity is still present in materials treated with Na vapor. An increase in pyridine uptake on Lewis sites in Na(v)/NaX samples is observed. This suggests that defect sites may also adsorb pyridine. It seems unlikely, however, that a single electron vacancy would permit a chemisorptive bond between pyridine and framework oxygen. The observation of increased pyridine uptake, therefore, is unexplainable by posing a single electron vacancy. If a two-electron vacancy is characteristic of the defect site, increased pyridine uptake would be expected. However, there is no way of knowing whether such species are present in these materials, for this type of site would be diamagnetic and EPR inactive. However, it is known that water reacts with these type of materials and produces a diamagnetic species.[13] Therefore, at present, no firm conclusions can be made about the exact nature of these defects. EPR and FTIR data before and after heating suggest that the nature of the holes and surrounding environment are quite different following heating.

The band at 3695 cm^{-1} observed in Na(v)/NaX zeolites (Figure 9) is significant in materials having Na_6^{5+} clusters. This band is indicative of water molecules hydrogen bonded to framework oxygen ions that were once associated with strong acidity and that the interactions between the free proton of hydrogen-bonded water and Na^+ ions give rise to this cation-dependent band at 3695 cm^{-1}.[50] These data are also consistent with the interaction of Na^+ with adsorbed water on the framework hole. This evidence suggests the presence of holes, and this band has been assigned to the presence of such defect sites. The presence of water in these materials is evident in the OH stretching region of the infrared.

Infrared analyses definitively show the presence of silicon hydride (Si−H) on the surface of the zeolite. The peak at 2208 cm^{-1} has been assigned to Si−H. A value of 2260 cm^{-1} has been reported for the formation of silicon hydride on the surface of alumina by a silanization process.[51] The assignment of this peak can easily be made because it is located in a very specific, characteristic region in the IR where only hydrides, cyanides, and carbynes are located. The latter two functional groups are not possible in these materials. Aluminum hydrides are known to occur at 1700 cm^{-1}.[52] ^1H MAS NMR data are also consistent with the formation of a Si−H species. Hydridic species might be expected to form in the presence of $H^\bullet$ species generated upon reaction of Brønsted sites or water with metallic sodium, as shown in eq 4. In addition, a reduction in the zeolite framework by Na^0, as evidenced by MAS NMR and X-ray diffraction, might facilitate the formation of Si−H species by creating available bonding sites on silicon.

The formation of hydridic species is enhanced with increasing temperature. Upon an increase in temperature, the band at 2208 cm^{-1} becomes sharper, more intense, and increasingly well-defined. This is evident by comparing the spectra of Figures 9 and 10.

The source of atomic hydrogen has been suggested to come from the reaction of Na vapor with Brønsted sites or from residual water in the zeolite,[23] although spectroscopic evidence for the formation of hydrides in zeolites has yet to be reported in ionic cluster formation reactions. In addition, it has been reported that $H^\bullet$ does not react with V-center holes, generated during cluster decomposition.[34]

These observations imply that the formation of silicon hydride during thermal decomposition of the clusters is a probable reaction. Sodium oxide might also form upon heating the Na cluster system. This may occur in the presence of oxygen at high (>100 °C) temperatures. Release of oxygen from such zeolites is known to occur at high temperatures.[38]

The modification of the zeolite structure by formation of hydridic species on the surface is likely to result in surface defect sites. The EPR signal at $g = 2.003$ in heated materials may correspond to such a defect site. A reduction of the zeolite framework may result either from metallic sodium or through the breakdown of ionic clusters. Both materials are easily oxidized; therefore, it is difficult to determine which species is responsible for the hydride reaction or if both species are acting synergistically with each other in this process.

Luminescence spectra of Figure 11 confirm the presence of an emitting species. We have assigned this species to a trapped electron in the Na_6^{5+} cluster. The transition observed in the luminescence might be due to interactions between two (or

more) ionic clusters located in adjacent sodalite cages, which has been suggested to occur,[33] or between the electron and surrounding nuclei. This subject was previously discussed (see discussion on EPR). A blue center has been associated with a highly energetic species and, more specifically, in similar metal ion clusters as trapped electrons. The color center and luminescence are lost upon heating these materials at 380 °C. This suggests that the cluster decomposes at higher temperatures and that the trapped electron is released from the cluster.

C. *Catalysis.* Catalytic and spectroscopic experiments suggest that the degradation of Na_6^{5+} ionic clusters in NaX zeolites greatly enhances catalytic cracking properties at high temperature. It is unlikely, however, that the clusters themselves are catalytically active. The negatively charged (formal charge) Na_6^{5+} clusters are unlikely to cause ring opening since literature studies suggest that ring opening occurs on positively charged sites.[29,53] Furthermore, Na_6^{5+} clusters are reported to exist only in the sodalite cages,[10,15,30] where cyclopropane cannot diffuse, based on size constraints of the molecule.[49] Finally, the clusters decompose before the onset of isomerization as shown by spectroscopic and catalytic studies.

Upon exposure to air or moisture for an extended period of time (>10 min), Na(v)/NaX loses its catalytic activity. This is consistent with data of Martens et al., who report that catalytic activity of such systems is extremely sensitive to oxygen and water molecules.[16]

Butene has been reported to isomerize to 2-butene with a high cis/trans ratio at 300 K over basic materials such as Na_2O.[54] Butene isomerization experiments studied here show that no reaction is observed up to 100 °C over Na(v)/NaX materials. This suggests that Na_2O is not the catalytically active site in this reaction. Furthermore, we know of no mechanism for the base catalysis of cyclopropane. c-C_3H_6 ring opening reactions occur through a carbenium ion intermediate and are known to occur typically over acid sites,[29,53] not over base sites. In addition, previous experiments showed that activity in cyclopropane isomerization reactions is drastically diminished upon exposure of acid zeolites to sodium vapor.[29] Sodium metallic particles have also been reported to be the active sites in the base catalysis of butene.[11,16]

Recently, Martens et al.[55] investigated zeolites containing sodium clusters as base catalysts for butene isomerization. From this study, it was suggested that framework oxygen anions in the neighborhood of intercrystalline neutral sodium clusters act as the active base site. Spectroscopic results form our studies suggest that O_2^- anions do not react with framework defect sites. Furthermore, butene isomerization reactions over sodium-treated materials prepared here show no catalytic activity at 300 K whatsoever.

Our results suggest that base catalysis is not a contributing factor in zeolites modified by sodium vapor. Further we have shown that zeolites containing excess sodium have diminished catalytic activities in c-C_3H_6 isomerization reactions. Although this may be a result of pore blockage, it also shows that sodium metal on the surface of the crystallite is inactive in c-C_3H_6 isomerization reactions.

Adsorption of cyclopropane on negatively charged centers such as hydrides is unlikely due to the fact that cyclopropane has high electron charge density in the center of the ring.[56] Previous mechanisms suggest that adsorption and reaction of c-C_3H_6 to C_3H_6 occurs over positively charged Brønsted sites.[29,53]

Iron impurities have been suspected to be catalytically active sites in zeolites.[27] The complete reduction of Fe^{3+} to Fe^0 with sodium occurs at high temperature and with the use of excess sodium.[57] EPR data show that Fe^0 is not observed in our systems, suggesting that Na vapor treatment conditions used here are relatively mild. This is consistent with XRD analyses and ^{27}Al MAS NMR studies which showed only slight degrees of dealumination of these materials. Furthermore, inductively coupled plasma analyses on NaX starting materials show less than 250 ppm Fe^{3+} impurity in these materials. These trace amounts of Fe^{3+} are unlikely to account for the high propylene conversions that were observed.

Partial reduction of Fe^{3+} to Fe^{2+} can occur at lower temperatures as shown in eq 6.

$$Fe^{3+} + Na^0 \rightarrow Fe^{2+} + Na^+ \qquad (6)$$

Certain transition metal ions are thought to be active sites for the isomerization of c-C_3H_6 at higher temperatures.[58] When excess sodium is applied, it is expected that reaction 6 would be driven to the right. If Fe^{2+} species were present and catalytically active, then the activity would be expected to increase with increasing sodium concentrations. Catalytic data suggest, however, that excess sodium causes complete poisoning of catalytically active sites, resulting in a total loss of catalytic activity.

The most plausible explanation for increased catalytic activity at high temperatures, therefore, is that defect sites created upon treatment with Na vapor or holes associated with Na_6^{5+} clusters catalyze c-C_3H_6 isomerization reactions. FTIR and NMR analyses show that desorption of tightly adsorbed water molecules to holes occurs upon heating at high temperatures. The desorption process results in an EPR active band at $g = 2.003$. Water associated with framework holes, prior to dehydration, is known to produce a diamagnetic material.[13] The complete desorption of adsorbed water (as evidenced by FTIR) frees up catalytically active holes at high temperatures and provides an oxidative center available for hydrocarbon conversion reactions. This is consistent with both the oxidation of naphthalene and the isomerization of cyclopropane on thermally treated Na(v)/NaX materials.

Holes on framework oxygen are stabilized between the aluminum and silicon atoms of the zeolite. Lewis sites associated with framework aluminum can further stabilize these defects. Substantial spectroscopic evidence from our studies suggests that the recombination of electrons (released during the thermal decomposition of ionic clusters) with framework holes does not occur at high temperature. The presence of O_2^- species suggests that it is more favorable for electrons to combine with molecular oxygen trapped in the zeolite than with the holes. This may be a result of the close proximity of free electrons to oxygen or due to a greater accessibility of mobile gas phase oxygen to electrons rather than to the holes on framework oxygen. The thermal generation of superoxide anions is energetically favorable. The spectroscopically characterized species generated upon heating of sodium ionic clusters support the existence of positively charged holes at high temperatures.

The generation of defect sites has been previously observed in the formation of ionic clusters via γ-irradiation.[23,25,26] The physicochemical changes observed in samples exposed to γ-irradiation have been explained in terms of trapped electrons, holes, lattice vacancies, and interstitial entities.[59] Changes in adsorption properties and catalytic activity which result from irradiation have been explained by two mechanisms.[60]

One theory involves a structurally unmodified system in which holes are formed as a result of irradiation which ionizes the surface of the material. The second involves a structurally modified system whereby γ-irradiation generates defect sites

on the surface of the material. In zeolites modified by sodium vapor, it appears that both theories might apply.

In our study, in the formation of positively charged holes, it is apparent that sodium ionic clusters are acting as reducing agents. Sodium can act as a reducing agent which can result in structural modification of the zeolite by creating a hydride species on the zeolite. We suggest that the formation of Si−H species is likely to result in the presence of defect sites possibly associated with the hydride.

Catalytically active holes and defect sites have been previously reported.[39,41,61] The concentration of induced defect sites on aluminosilicate frameworks has been directly related to catalytic activity in cumene cracking.[62] A charge transfer reaction has been invoked which involves the generation of carbenium ions over positively charged holes.[39] Similarly, the ring opening of conjugated radical cation systems has been attributed to positively charged holes.[40] The catalytic isomerization of c-C_3H_6 in our system is a result of positively charged holes that alter the adsorptive and catalytic properties of zeolites.

Differences in activation energies between NaX and Na(v)/NaX may be explained in terms of differences in mechanisms resulting from the presence of different types of active sites in the two systems. It is clear that activity in NaX is attributed to low initial Brønsted acidity present in these materials. Large E_a values for Na(v)/NaX may be a result of stronger interactions of cyclopropane with holes. c-C_3H_6 may chemisorb more strongly to the holes, thereby increasing the heats of sorption, reaction, and desorption, which result in increased activation energies. Higher reaction temperatures required to activate Na(v)/NaX catalysts are also consistent with higher activation energies.

Deactivation of NaX occurs rapidly within the first 30 min time on stream, whereas the Na(v)/NaX catalysts do not deactivate at higher temperatures. This suggests that catalytic intermediates formed on the surface readily desorb on Na(v)/NaX, whereas intermediates may react further and oligomerize or polymerize on the Brønsted sites of NaX.

V. Conclusions

Ionic sodium clusters having the formula Na_6^{5+} have been produced in NaX zeolites by a CVD process from sodium metal. Na_6^{5+} clusters have been determined to be present in Na vapor-treated NaX zeolite and characterized by EPR, MAS NMR, FTIR, and luminescence. EPR signals for Na_6^{5+} clusters exhibit hyperfine structure and g values characteristic of holes on framework oxygen atoms of the zeolite are present in these materials. Exposure of Na_6^{5+} clusters to air results in three EPR bands which have been assigned to the superoxide ion adsorbed on Na^+ cations. Heating of Na_6^{5+} clusters results in decomposition of the clusters and an EPR signal corresponding to O_2^-. Oxygen serves as an electron trap, preventing the free electron from recombining with existing holes upon decomposition of the clusters.

Heating of ionic clusters results in structural modification of the zeolite surface. NMR and FTIR results suggest the formation of Si−H species on the surface of the zeolite, particularly at higher temperatures. This structural modification may lead to defect sites on the catalyst. Structural modification, in turn, may change the environment, properties and the location of framework defect sites. ^{23}Na NMR reveals the presence of Na_6^{5+} clusters in close proximity to Na^+ in sites I′, II, and III, but not in site I. Metallic sodium also appears to be closely associated with Na_6^{5+} ionic clusters.

Pyridine adsorption studies have shown that zeolites exposed to sodium vapor lose Brøsted acidity and that ionic clusters, and resulting defects, are not acidic. Lewis site adsorption significantly increases for Na vapor-modified materials. FTIR data also suggest the presence of a strong adsorption site in these materials that has been assigned to holes in the material.

Catalytic results for cyclopropane isomerization reactions show that conversion to propylene increases from 5% to 85% in materials containing Na_6^{5+} clusters. Catalytic activity in the supercages of Na(v)/NaX has been associated with the formation of Na_6^{5+} ionic clusters. Ionic clusters themselves have been shown not to be catalytic centers. Positively charged holes or defect sites, formed in the zeolite upon treatment with sodium, have been suggested to be responsible for c-C_3H_6 ring opening.

EPR experiments of sublimed naphthalene on sodium-treated NaX materials suggest that positively charged defect sites formed upon thermal treatment of ionic clusters are different than those produced upon ionic cluster formation. Catalytically active sites are produced at high temperatures. Adsorption of water to holes following cluster formation prevents catalytic activity. Thermal activation of holes changes the environment surrounding these defect sites and results in catalytic oxidative centers on Na(v)/NaX materials.

Treatment of NaX zeolite with excess sodium resulted in a total loss of catalytic activity. EPR signals corresponding to sodium ionic clusters or holes were not observed in samples prepared with excess sodium. Trace amounts of iron impurities also do not appear to be responsible for catalytic activity.

Activation energies for c-C_3H_6 reactions are approximately 3 kcal/mol greater for Na(v)/NaX than NaX. This has been explained in terms of stronger interactions that might exist between adsorption sites in Na vapor-modified zeolites and cyclopropane.

Acknowledgment. The authors thank Roberto N. DeGuzman for collecting EPR data. We also thank Dr. Lennox E. Iton at Argonne National Laboratory for helpful discussions. We gratefully acknowledge the Department of Energy, Office of Basic Energy Sciences, Division of Chemical Sciences and Texaco, Inc., for support of this research.

References and Notes

(1) Bhatia, S.; Beltramini, J.; Do, D. D. *Catal. Rev.—Sci. Eng.* **1989**, *31*, 455.
(2) Fritz, P. O.; Lunsford, J. H. *J. Catal.* **1989**, *118*, 85.
(3) Beyerlein, R. A.; McVicker, G. B.; Yacullo, L. N.; Zeiemiak, J. J. *Proc. ACS Meet. Div. Petrol. Chem., New York* **1986**, *31*, 190.
(4) Barrault, J.; Renard, C. *Appl. Catal.* **1985**, *14*, 133.
(5) Sinfelt, J. H.; Carter, J. L.; Yates, D. J. C. *J. Catal.* **1972**, *24*, 283.
(6) Kasai, P. H. *J. Chem. Phys.* **1965**, *43*, 3322.
(7) Rabo, J. A.; Angell, C. L.; Kasai, P. H.; Schomaker, V. *Discuss. Faraday Soc.* **1966**, *41*, 328.
(8) Ben Taarit, Y.; Naccache, C.; Che, M.; Tench, A. J. *J. Chem. Phys. Lett.* **1973**, *24*, 41.
(9) Westphal, U.; Geismar, G. *Z. Anorg. Allg. Chem.* **1984**, *508*, 165.
(10) Harrison, M. R.; Edwards, P. P.; Klinowski, J.; Thomas, J. M. *J. Solid State Chem.* **1984**, *54*, 330.
(11) Martens, L. R. M.; Grobet, P. J.; Vermeiren, W. J. M.; Jacobs, P. A. *Stud. Surf. Sci. Catal.* **1987**, *31*, 531.
(12) Xu, B.; Kevan, L. *J. Chem. Soc., Faraday Trans.* **1991**, *87*, 2843.
(13) Yoon, K. B.; Kochi, J. K. *J. Chem. Soc., Chem. Commun.* **1991**, 510.
(14) (a) Anderson, P. A.; Singer, R. J.; Edwards, P. P. *J. Chem. Soc., Chem. Commun.* **1991**, 914. (b) Anderson, P. A.; Edwards, P. P. *J. Chem. Soc., Chem. Commun.* **1991**, 915.
(15) Edwards, P. P.; Harrison, M. R.; Klinowski, J.; Ramdas, S.; Thomas, J. M.; Johnson, D. C.; Page, C. J. *J. Chem. Soc., Chem. Commun.* **1984**, 982.
(16) Martens, L. R. M.; Grobet, P. J.; Jacobs, P. A. *Nature* **1985**, *315*, 568.
(17) Fejes, P.; Hannus, I.; Kiricsi, I.; Varga, K. *Acta Phys. Chem.* **1978**, *24*, 119.

(18) Fejes, P.; Kiricsi, I.; Hannus, I.; Tihanyi, T.; Kiss, A. In *Catalysis by Zeolites*; Imelik, B., et al., Eds.; Elsevier: Amsterdam, 1980; pp 135–140.
(19) Kiricsi, I.; Hannus, I.; Kiss, A.; Fejes, P. *Zeolites* **1982**, *2*, 247.
(20) Park, Y. S.; Lee, Y. S.; Yoon, K. B. *J. Am. Chem. Soc.* **1993**, *115*, 12220.
(21) Anderson, P. A.; Barr, D.; Edwards, P. P. *Angew. Chem.* **1991**, *103*, 1511; *Angew. Chem., Int. Ed. Engl.* **1991**, *30*, 1501.
(22) Srdanov, V. I.; Haug, K.; Metiu, H.; Stucky, G. D. *J. Phys. Chem.* **1992**, *96*, 9039.
(23) Lui, X.; Thomas, J. K. *Langmuir* **1992**, *8*, 1750.
(24) Lui, X.; Thomas, J. K. *Chem. Phys. Lett.* **1992**, *5*, *6*, 555.
(25) Abou-Kais, A.; Vedrine, J. C.; Massardier, J. *J. Chem. Soc., Faraday Trans. 1* **1974**, *71*, 1697.
(26) Abou-Kais, A.; Vedrine, J. C.; Massadier, J.; Dalmai-Imelik, G. *J. Chem. Soc., Faraday Trans. 1* **1973**, *70*, 1039.
(27) Sinfelt, J. H. *Bimetallic Clusters*; John Wiley & Sons: New York, 1983.
(28) Sinfelt, J. H. *Science* **1977**, *195*, 641.
(29) Simon, M. W.; Efstathiou, A. M.; Bennett, C. O.; Suib, S. L. *J. Catal.* **1992**, *138*, 1.
(30) Xu, B.; Chen, X.; Kevan, L. *J. Chem. Soc., Faraday Trans.* **1991**, *87*, 3157.
(31) Guy, S. C.; Edwards, P. P. *Chem. Phys. Lett.* **1982**, *86*, 150.
(32) Walsh, W. M.; Rupp, L. W.; Schmidt, P. H. *Phys. Rev. Lett.* **1981**, *16*, 181.
(33) Anderson, P. A.; Edwards, P. P. *J. Am. Chem. Soc.* **1992**, *114*, 10608.
(34) Vedrine, J. C.; Abou-Kais, A.; Massardier, J.; Dalmai-Imelik, G. *J. Catal.* **1973**, *29*, 120.
(35) Kasai, P. H.; Bishop, R. J. *J. Phys. Chem.* **1973**, *77*, 2308.
(36) Kaisi, P. H.; Bishop, R. J. *Adv. Chem. Ser.* **1976**, *171*, 350.
(37) Pfeffer, R. C. *J. Appl. Phys.* **1985**, *57*, 5176.
(38) Suib, S. L.; Morse, B. E. *Langmuir* **1989**, *5*, 1340.
(39) Shih, S. *J. Catal.* **1983**, *79*, 390.
(40) Vincow, G. *Radical Ions*; Interscience: New York, 1968.
(41) *Handbook of Chemistry and Physics*, 64th ed.; CRC Press: Boca Raton, FL, 1983; p E-71.
(42) Shida, T.; Egawa, Y.; Kubodera, H. *J. Chem. Phys.* **1980**, *73*, 5963. Shih, S. *J. Phys. Chem.* **1975**, *79*, 2201.
(43) Corio, P. L.; Shih, S. *J. Catal.* **1970**, *18*, 126.
(44) Ratcliffe, C. I.; Ripmeester, J. A.; Tse, J. S. *Chem. Phys. Lett.* **1985**, *120*, 427.
(45) Hunger, M.; Freude, D.; Pfeifer, H. *Catal. Today* **1988**, *3*, 507.
(46) Hayashi, S.; Hayamizu, K.; Yamamoto, O. *Bull. Chem. Soc. Jpn.* **1987**, *60*, 105.
(47) McMurray, L.; Holmes, A. J.; Kuperman, A.; Ozwi, G. A.; Ozkar, S. *J. Phys. Chem.* **1991**, *95*, 9448.
(48) Simon, M. W.; DeGuzman, R. N.; Suib, S. L. Unpublished results.
(49) Efstathiou, A. M.; Borgstedt, E. v. R.; Suib, S. L.; Bennett, C. O. *J. Catal.* **1992**, *135*, 135.
(50) Ward, J. W. *In Zeolite Chemistry & Catalysis*; Rabo, J. A., Ed.; American Chemical Society: Washington, DC, 1976; p 187.
(51) Pesek, J. J.; Sandoval, J. E.; Su, M. *J. Chromatogr.* **1993**, *690*, 95.
(52) Fraser, G. W.; Greenwood, N. N.; Straughan, B. P. *J. Chem. Soc.* **1963**, 3742.
(53) Jacobs, P. A. *Carbogenionic Activity of Zeolites*; Elsevier: Amsterdam, 1977.
(54) Noumi, H.; Misumi, T.; Tsuchiya, S. *Chem. Lett.* **1978**, 493.
(55) Martens, L. R.; Vermeiren, W. J.; Huybrechts, D. R.; Grobet, P. J.; Jacobs, P. A. In *Proceedings, 9th International Congress on Catalysis, Calgary, 1988*; Phillips, M. J., Ternan, M., Eds.; The Chemical Institute of Canada: Ottawa, 1988; Vol. 1, p 420.
(56) Roginski, S. Z.; Rathmann, J. *J. Am. Chem. Soc.* **1933**, *55*, 2800.
(57) Lee, J. B. *J. Catal.* **1981**, *68*, 27.
(58) Bonnevoiot, L.; Olivier, D.; Che, M. *J. Mol. Catal.* **1983**, *21*, 415.
(59) Muha, G. M. *J. Phys. Chem.* **1966**, *70*, 1390.
(60) Kohn, H. W.; Taylor, E. H. *Actes du 2eme Congres Catalyse*; Technip: Paris, 1960; p 1461.
(61) Hays, J. D.; Bunbar, R. C. *J. Phys. Chem.* **1979**, *83*, 3183.
(62) Vedrine, J. C.; Barthomeuf, D.; Dalmai, G.; Trambouze, Y.; Imelik, B.; Prettre, M. *Compt. Rend. C* **1968**, *267*, 118.

JP942851X